Molecular Informatics

Conformational Properties and Energetic Analysis of Aliskiren in Solution and Receptor Site

Journal:	*Molecular Informatics*
Manuscript ID:	minf.201100077
Wiley - Manuscript type:	Full Paper
Date Submitted by the Author:	10-May-2011
Complete List of Authors:	Mavromoustakos, Thomas; University of Athens, Chemistry Polit, Aggeliki; NHRF/IOPC Leonis, George; NHRF/IOPC Tzoupis, Charalampos; NHRF/IOPC Ntountaniotis, Dimitris; University of Patras, Chemistry Reis, Heribert; NHRF/IOPC Papadopoulos, Manthos; NHRF/IOPC Grdadolnik, Simona; National Institute of Chemistry
Keywords:	Conformation analysis, Computational chemistry, NMR spectroscopy

Conformational Properties and Energetic Analysis of Aliskiren in Solution and Receptor Site

A. Politi[1,2], G. Leonis[2*], H. Tzoupis[1,2], D. Ntountaniotis[3], H. Reis[2], M. G. Papadopoulos[2], S. G. Grdadolnik[4,5], T. Mavromoustakos[1,2*]

[1]*University of Athens, Department of Chemistry, Laboratory of Organic Chemistry, Zographou, Athens 15771, Greece*

[2]*National Hellenic Research Foundation, Institute of Organic and Pharmaceutical Chemistry, 48 Vas. Constantinou, Athens 11635, Greece*

[3]*Department of Chemistry, University of Patras, Patras 26500, Greece*

[4]*Laboratory of Biomolecular Structure, National Institute of Chemistry, Hajdrihova 19, SI-1001 Ljubljana, Slovenia*

[5]*EN-FIST Centre of Excellence, Dunajska cesta 156, SI-1000 Ljubljana, Slovenia*

Corresponding authors:

T. Mavromoustakos

University of Athens, Department of Chemistry, Laboratory of Organic Chemistry, Zographou, Athens 15771, Greece
*email: tmavrom@chem.uoa.gr

G. Leonis

National Hellenic Research Foundation, Institute of Organic and Pharmaceutical Chemistry, Vas. Constantinou 48, Athens 11635, Greece
*e-mail: gleonis@eie.gr

Abstract

Aliskiren is the first orally active, direct renin inhibitor to be approved for the treatment of hypertension. Its structure elucidation and conformational analysis were explored using 1D and 2D NMR spectroscopy, as well as random search and molecular dynamics (MD) simulations. MD calculations of aliskiren were also performed at the receptor site, in order to reveal its molecular basis of action. It is suggested that aliskiren binds in an extended conformation and is involved in several stabilizing hydrogen bonding interactions with active site (Asp32/255, Gly34) and other binding-cavity (Arg74, Ser76, Tyr14) residues. Of paramount importance is the finding of a loop consisting of residues around Ser76 that determines the entrapping of aliskiren into the active site of renin. The details of this mechanism will be the subject of a subsequent study. Molecular mechanics Poisson-Boltzmann surface area (MM-PBSA) free energy calculations for the aliskiren-renin complex provide insight into the binding mode of aliskiren by identifying van der Waals and nonpolar contribution to solvation as the main components of favorable binding interactions, and may lead to the rational design of molecules with optimized pharmacological profile.

1 Introduction

Among all the systems that regulate cardiovascular, renal and other metabolic functions, endocrine renin–angiotensin–aldosterone system (RAAS) is the most important.[1] RAAS activation is stimulated by signals such as drop in blood pressure, loss of blood volume, or reduction in plasma sodium concentration. These signals trigger the release of renin—a highly specific and selective aspartic protease—, which cleaves angiotensinogen to produce the inactive decapeptide angiotensin I.[2] Angiotensin I is next converted by angiotensin-converting enzyme (ACE) to the active peptide angiotensin II, which increases the blood pressure either by causing blood vessels to compress or by stimulating the secretion of the hormone aldosterone. Since the rate-limiting step in this cascade is determined by renin (catalyzing the cleavage of the Leu10-Val11 amide bond of angiotensinogen) to produce angiotensin I, inhibition of this step would be an effective therapeutic scheme against hypertension.[3,4]

Angiotensinogen is the only known substrate for renin;[2,5] this renders renin of extreme importance regarding selectivity and enzyme specificity. Mature renin is a 340-amino acid, pepsin-like enzyme. The active site of the protein is a deep cleft between the N– and the C–terminal domains to which the inhibitors bind in an extended conformation.[6,7] Similarly to other aspartic proteases (eg. HIV-1 protease), the active site of renin consists of two catalytic triads, Asp32/215, Thr33/216, and Gly34/217.

During the past decades many pharmaceutical companies have developed renin inhibitors. Most of them were based on peptidic or peptidomimetic scaffold, which confers low stability and poor oral bioavailability in humans.[8] Molecular modeling

and X-ray crystal structure determination of the active site of renin have led to the identification of new renin inhibitors with reduced peptidic character and smaller size.[9,10] Aliskiren (Figure 1) was approved in 2007 by the FDA as the first orally active, direct renin inhibitor for the treatment of hypertension.[8,11,12] It has four chiral centers and binds directly to the binding pocket of renin, thus preventing the conversion of angiotensinogen to angiotensin I. A representative structure of aliskiren inside renin is presented in Figure S1. A highly potent inhibitor for human renin, aliskiren has IC_{50} in the low nM range (0.6 nM) and biological half-life ≈ 24 h.[13]

As a continuation of our effort to obtain information on the structural requirements of renin inhibitors for enhanced activity, we initiated a study on the conformational properties of aliskiren.[14] To explore the conformational diversity of molecules, a variety of efficient conformational searching methods are available, e.g. Monte Carlo (MC) and Molecular Dynamics (MD).[15] Additionally, free-energy simulations employ structural information to obtain a quantitative estimation of binding affinities and their critical components.[16-18] Among these approaches, free-energy perturbation (FEP) and thermodynamic integration (TI) techniques, combine statistical mechanics with the thermodynamic cycle to compute absolute and relative free energies of binding.[19-22] A reliable method to estimate the absolute binding free-energy change in protein systems is the molecular-mechanics Poisson-Boltzmann surface area (MM-PBSA).[23-25] This method is based on a combination of molecular mechanics (MM) energies for the solute with a continuum solvation model (Poisson-Boltzmann). Normal mode analysis supplements the MM-PBSA method to approximate more accurately the total free energies. In this study, MD, MC, quantum mechanical (QM) and MM-PBSA calculations, in combination with NMR spectroscopy, have been

performed to explore the conformational properties and the energetics of aliskiren in solution, as well as for aliskiren bound to renin.

The structure of aliskiren in dimethylsulfoxide (DMSO) using NMR spectroscopy and MD calculations appears very mobile, yet mainly extended, thus rationalizing the use of the X-ray crystallographic structure as the starting point for an MD simulation of aliskiren inside renin. A more thorough understanding of the enzyme's behavior may be gained after the study of dynamic properties such as the flexibility of the systems, dominant hydrogen bonding (HB) interactions and conformational changes inside the binding cavity. It is suggested that although aliskiren remains relatively flexible upon binding, it keeps its extended conformation and forms a hydrogen bonding network, which involves interactions between aliskiren and binding-cavity residues such as Asp32/215, Gly34 (active site), and Tyr14, Arg74, Ser76. Of particular interest is the role of a loop consisting of residues that define the sequence around Ser76: it belongs to the outer region of renin, on top of the active site and it is implicated in modulating ligand-access to the cavity. It appears increasingly flexible in the unbound form of renin, rapidly alternating from "closed" to "open" states. However, upon aliskiren binding, its flexibility reduces significantly due to HB interactions that stabilize aliskiren inside the protease. Additionally, binding-energy calculation studies using the MM-PBSA algorithm shed light to the molecular basis of aliskiren binding at the active site of renin and may lead to the rational design of new molecules. Our binding free-energy calculations are in agreement with the experimental results, further suggesting that van der Waals interactions along with nonpolar contribution to solvation act most favorably to aliskiren binding.

2 Experimental

2.1 Materials

Deuterated DMSO-*d*6 and ultra precision NMR tubes Wilmad 535–5 mm (SPINTEC ROTOTEC) were used for the NMR experiments. Aliskiren was kindly offered by the Novartis Pharmaceutical company.

2.2. Methods

2.2.1 Nuclear Magnetic Resonance Spectroscopy

NMR spectra were recorded on Varian 600 spectrometer. Chemical shifts are given on a δ (ppm) scale using TMS as an internal standard. The 2D experiments (HSQC, HMBC, COSY, and NOESY) were performed using standard Varian pulse sequences.

2.2.2 Conformational Analysis

Monte Carlo Simulations of Aliskiren in DMSO: MC studies were performed using QUANTA software of Molecular Simulation Incorporated (MSI).[26] The CHARMm force field[27] was applied for the potential energy calculations and all studies were run using a dielectric constant ε = 45 to simulate DMSO environment. DMSO provides an amphiphilic environment, mimicking the physiological conditions at the receptor binding site.[28,29] Aliskiren was first minimized with steepest descent and then with Newton–Raphson algorithms using an energy tolerance of 0.001 kcal $mol^{-1}A^{-1}$. MC searches were performed for energy optimization with 0.001 convergence

threshold. 5000 steps were run and the conformers obtained were classified as "closed" or "open" structures.

Molecular Dynamics of Aliskiren in DMSO: Simulations were performed using the SANDER[30] module under the AMBER 11 software package.[31] The initial structure for the aliskiren molecule was taken from the crystal structure of renin-aliskiren complex [Protein Data Bank (PDB) ID code: 2V0Z)],[32] and it was constructed with the ANTECHAMBER module (using the general AMBER GAFF force field).[33,34] The atomic partial charges were calculated with the AM1-BCC method.[35] The solvation in DMSO was obtained using the tLEaP module of AMBER by adding 442 DMSO molecules. A pre-equilibrated DMSO box was obtained from the Bryce group.[36] Truncated octahedral periodic boundary conditions were applied, with a cutoff distance of 12 Å.

The starting step was the minimization of the system over 5000 steps by keeping aliskiren atoms constrained. For the first 2500 steps the steepest descent method was used, while for the next 2500 steps the conjugate gradient algorithm was employed. The system was allowed to relax further for another 5000 steps by removing the constraints from aliskiren. The next procedure involved the gentle heating from 0 K to 300 K in the NVT ensemble, over a period of 50 ps; aliskiren was also constrained by a force of 10 kcal mol^{-1} $Å^{-2}$. A 200 ps equilibration period at constant pressure followed after allowing aliskiren and DMSO atoms to move freely. Finally, MD simulation of the system was performed for 200 ns, using a Langevin dynamics temperature scaling[37] with a collision frequency of 2.0 ps^{-1}. For the thermalization, equilibration and MD runs, the SHAKE algorithm[38] was employed for all atoms covalently bonded to hydrogen atoms, thus allowing for a time step of 2 fs. All van der Waals interactions were calculated within a distance cutoff of 15 Å.

Clustering: The clustering was performed using the hierarchical algorithm from the MOIL-View version 10.0 suite, written by Carlos Simmerling.[39] As the distance metric for the clustering a 2.5 Å RMSD cutoff was introduced to classify 100,000 conformations. The representative structures produced by the clustering were used for further analysis.

Quantum Mechanical Calculations: The coordinates of the representative structures obtained before were used to perform B3LYP/6-31G(d)[40] geometry optimization calculations in gas phase and in DMSO solution with the Gaussian 09 program.[41]

Molecular Dynamics of Aliskiren Inside Renin in Water: MD simulations for aliskiren-renin complex in explicit solvent have been also carried out with AMBER 11. Initial structures for the protein were taken from crystallographic data: The wild-type sequence of the aliskiren-bound form of renin was obtained from the dimeric protein-inhibitor complex (PDB ID: 2V0Z). A second protease structure was considered (PDB ID: 2V10)[32] to test the effect of a different initial conformation to our calculations. The analysis of the trajectories obtained did not produce significant differences, thus we chose to report here only results referring to complex 2V0Z. After removing the inhibitor, the apo crystal structure 2V0Z was also subjected to MD analysis to account for the behavior of the unbound renin. Only the one monomer of 2V0Z was considered for obtaining initial coordinates for the complex. Any further protein modifications, including addition of hydrogen atoms and creation of disulfide bonds (between cysteines 45-50, 206-210 and 249-282) were performed with LEaP in AMBER. The active site was considered monoprotonated (Asp32), according to previous experimental and theoretical studies.[42,43] For renin, the atomic partial charges, bond lengths, bond angles, dihedral angles, their respective force constants, and van der Waals parameters were represented by the modified AMBER ff99SB

force field.[44] Force field parameters and partial charges for aliskiren were assigned as follows: missing hydrogen atoms were added with the program *reduce*,[45] after obtaining the coordinates of aliskiren from 2V0Z. Next, the geometry of aliskiren was optimized with the HF/6-31G* basis set (Gaussian 09). Finally, ANTECHAMBER was used to derive the RESP atomic partial charges[46] for aliskiren, and the general AMBER GAFF force field was employed to obtain the force field parameters for the inhibitor. The explicit solvent model was used (in all systems) to model the effects of solvation. Simulations used the TIP3P water model[47] and each structure was solvated in a truncated octahedral water box to allow for at least 10 Å between each atom of the protein and the edge of the periodic box. Crystal water molecules were kept in the structure, and approximately 11500 water molecules were added with LEaP. Also, seven Na^+ counterions were added to neutralize the system.

A four-step energy minimization process with the steepest descent method was used to direct the system towards an energetically favorable conformation. The first step kept the solute (either renin-aliskiren complex or renin itself) practically fixed with a harmonic force constant of 500 kcal mol^{-1} $Å^{-2}$, while the water molecules were allowed to relax. Next, the strength of the restraint was gradually reduced in two steps to 10 kcal mol^{-1} $Å^{-2}$ and eventually to 2 kcal mol^{-1} $Å^{-2}$. Finally, the restraint was removed, to allow all atoms to move freely. Each of the four steps was realized in 3000 cycles with a cutoff of 20 Å. The temperature of the system was then gradually raised from 0 K to 300 K under constant volume, over a period of 100 ps. The SHAKE algorithm was applied to constrain all bond lengths involving hydrogen to their equilibrium distance, and a 2 fs time step was used. The Langevin thermostat with a collision frequency of 2.0 ps^{-1} was then used to keep the temperature constant. A restraint of 10 kcal mol^{-1} $Å^{-2}$ was also applied to the solute. The same restraint was

kept for the next 100 ps of equilibration in the NPT ensemble. A final equilibration stage of 100 ps was performed with all atoms of the system unrestrained. The subsequent MD calculations lasted for 15 ns, for each system (aliskiren-bound complex and renin itself). The SHAKE algorithm, Langevin thermostat along with the 10 Å nonbonded cutoff were applied during all previous heating and equilibration periods.

For all trajectories obtained, further analysis (hydrogen bonding, distance and Cα atomic fluctuation calculations, RMSD calculations) was realized with the ptraj module under AMBER. For the HB calculations, a 3.5 Å donor-acceptor distance cutoff along with a cutoff of 120° for the donor-hydrogen-acceptor angle were applied.

Application of Molecular Mechanics Poison-Boltzmann Surface Area Methodology to Calculate the Binding Free Energy of the Complex: For the renin-aliskiren system, the change in the binding free energy during the complexing (ΔG_{bind}) drives the binding process.

Initially, 1500 MD snapshots (equally spaced at 10 ps intervals) of the protein-aliskiren complex (stripped of water molecules and counterions) were considered. This spacing would be sufficiently far apart that the structures are uncorrelated (as required), yet an adequate population of structures is obtained to ensure a relatively low statistical error.[48] Based on the assumption that conformational changes are not significant upon binding, all snapshots were obtained from the trajectory of the complex (instead of running three independent simulations for renin, aliskiren and complex), according to the "single trajectory approach".[24] For each snapshot a free

energy for the complex, aliskiren and renin is calculated, and the total binding free energy ΔG_{bind} is computed using the following general equation:

$$\Delta G_{bind} = G_{complex} - (G_{renin} + G_{aliskiren}) \quad (1)$$

$G_{complex}$, G_{renin} and $G_{aliskiren}$ are the energies for the complex, the receptor and the ligand, respectively. The binding energy can be expressed as a combination of enthalpic and entropic contributions:

$$\Delta G_{bind} = \Delta H - T\Delta S \quad (2)$$

The enthalpic term in eq. 2 is calculated as:

$$\Delta H = \Delta G_{MM} + \Delta G_{solv} \quad (3)$$

where ΔG_{MM} defines the molecular mechanical (MM) free-energy change upon complex formation in the gas phase, and ΔG_{solv} is the solvation free energy.

ΔG_{MM} is further divided into Coulomb electrostatic interaction and van der Waals interaction terms:

$$\Delta G_{MM} = \Delta G_{ele} + \Delta G_{vdW} \quad (4)$$

For these nonbonded terms no cutoff was applied during the simulation. Furthermore, the solvation term of equation (3) is defined as a sum of polar (ΔG_{PB}) and nonpolar (ΔG_{NP}) contributions:

$$\Delta G_{solv} = \Delta G_{PB} + \Delta G_{NP} \quad (5)$$

The polar term of the energy was calculated by solving the Poisson-Boltzmann equation (PB method)[49] using the PBSA module of the AMBER suite, and the nonpolar contribution to the solvation free energy was determined as a function of the solvent-accessible surface area (SASA):[50-51]

$$\Delta G_{NP} = \gamma \mathrm{SASA} + \beta \quad (6)$$

In the above equation, the standard values for surface tension γ= 0.00542 kcal mol^{-1} Å^{-2} and for offset β= 0.92 kcal mol^{-1} were used.[51] A probe radius of 1.4 Å was considered. The dielectric constant for the solute was 1.0, and the solvent dielectric constant was 80.0. ΔG_{NP} was computed via eq. 6, with the linear combinations of pairwise overlaps (LCPO) method.[52]

Finally the entropic term $-T\Delta S$ (eq. 2) was calculated by normal mode analysis using the NMODE module[53,54] from AMBER, over only 150 equally spaced snapshots in order to save computational time. The entropy change is divided in translational, rotational, and vibrational contributions:

$$\Delta S = \Delta S_{trans} + \Delta S_{rot} + \Delta S_{vib} \quad (7)$$

3 Results and discussion

3.1 Structure Elucidation of Aliskiren

The assignment of aliskiren was achieved using DMSO-d_6 and 1D and 2D NMR experiments. The integration of the peaks provided evidence of the exact number of protons that constitute the aliskiren structure. 2D COSY and 2D NOESY experiments in combination with heteronuclear 2D HSQC and 2D HMBC experiments aided in the assignment of the protons and carbons that aliskiren bears in its structure. Figure 2 shows the ^{1}H NMR and ^{13}C NMR spectra in DMSO-d_6 with labeled protons and carbons as shown in Figure 1. Table 1 contains the ^{1}H and ^{13}C assignment of aliskiren in DMSO-d_6. 2D COSY, NOESY, HSQC and HMBC spectra are provided in supplementary material (Figures S2-S5). A representative table explaining the HSQC and HMBC spectra is also provided in the supplementary material (Table S1). The strategy followed for the assignment of aliskiren in DMSO-d_6 is briefly explained below.

The assignment was initiated with amide proton (CONH), which resonates at low field 7.52 ppm and has triplet multiplicity because it couples with the two vicinal protons 5α and 5β. CONH has spatial correlation with peaks resonated at 2.23, 1.00, 1.64 and 0.82 ppm, which are directly assigned to H7, H3/H4, H8 and H9/H10, respectively. H7 through bond correlations leads also to the assignments of H8, H9/H10, H11, H12, H13, H14, H15, H19, H16, H17/18. H11 are diasterotopic and appear as H11α and H11β with distinct chemical shifts. HMBC shows that C6 is

correlated through NH, H5, H7 and H11. This confirms the assignment of H11 and leads to the assignment of H5. Through COSY, H2 and H3/4 can be unambiguously assigned. Peaks at low field of 6.80 ppm and 7.16 ppm correspond to two protons and show COSY. These are assigned to CONHα and CONHβ. A peak at 7.16 ppm shows NOE with another peak at 1.02 ppm confirming the assignment of H3/4 protons. HMBC spectrum shows correlations of C1 with protons CONHα and CONHβ, H5α, H5β and H3/H4. Diastereotopic H19 (H19α and H19β) have spatial correlation with aromatic protons H21 and H25. These are easily differentiated because H21 is correlated through bond with H22. H29 and H30 appear as singlet's. H27 is quintet and has COSY with H28 and H26. HMBC shows correlation between C24 and H25, H26 and thus H26 is differentiated from H28. The carbons bearing protons are assigned from HSQC and quaternary carbons from HMBC. C23 has correlations with H22, H21 and H30 and C20 correlates with H25, H21, H19α and H19β, thus completing the assignment of all protons and carbons.

3.2 Conformational Analysis of Aliskiren in DMSO-d6

The most important NOEs observed in aliskiren that determine its conformational properties are quantified and are shown in Table 2. Random sampling and MD simulations were applied to the minimized structure of aliskiren in order to reveal more conformers that satisfy NOEs data. These conformers were compared with the crystallographic structure of aliskiren to identify the similarities and differences in the pharmacophoric segments. More specifically, the following conformational features were sought to be studied: (a) orientation of methoxy propoxy chain in relation to the benzene ring and the rest of the molecule (defined by τ_4-τ_8, Figure 1); (b) conformation and flexibility of the terminal segment (defined by τ_2, τ_3 and τ_9-τ_{31}); (c)

orientation and interactions of amine and hydroxyl groups as well as of the methoxy group (τ_1).

The strategy used in the conformational analysis was as follows: A random sampling and MD analysis were performed without using any constraints. The cluster analysis gives low energy conformers that reflect upon the flexibility of the molecule. Among the diverse conformers that usually are derived from flexible molecules as aliskiren appears to be, we would select the one that fits best the NOEs. This would serve as an initiative structure for performing docking calculations. The MD calculations will also provide us information about the stability of the structure that best fits NOEs and its conformer similarities and differences with crystallographic structure of aliskiren.

3.2.1 Random Sampling

Random sampling analysis considered 1000 conformers, which are minimized and classified into "open" and "closed" structures. Some characteristics of these low energy structures are briefly described below in order to show their versatility. In one group of molecules the terminal segment presented spatial proximity with the methoxy group. In another group of molecules the methoxy propoxy group was in close spatial vicinity with isopropyl group adjacent to the amide bond. Isopropyl groups appeared with different orientation. Finally, in a class of compounds the amide group orients towards the benzene ring. Six representative conformations are shown in Figure S6. The conclusion from this conformational analysis is that aliskiren is a highly flexible molecule as expected, and can adopt extended and packed or "bent" conformations.

3.2.2 Molecular Dynamics of Aliskiren in DMSO and Clustering

The cluster analysis on the MD trajectory of aliskiren in DMSO produced 2 major clusters. Cluster 1 (73 % populated) suggests an extended ("open") conformation for aliskiren (Figure 3a, red), whereas cluster 2 (27 % populated) denotes a "bent" structure (Figure 3a, green). The coordinates of the representative structures of each cluster were used for further QM optimizations and distance calculations. The analysis of the distances derived from the *ab initio* methods revealed similarities with NMR experimental data and are summarized in Table 3. It is evident from the data that both structures do not have significant differences with the NMR data. Also, it is evident from the mean relative errors that deviations between the gas and solvated phase of the aliskiren are minor. The extended structure appears almost identical in the gas and solvated states, as shown by the mean relative errors (MRE) to the experimental values: for cluster 1 the MRE is 0.18 for the conformation in the gas phase, and 0.17 for the conformation in the solvated state. For the representative structure of cluster 2, the gas and solvated phases show small differences (MRE 0.16 and 0.23, respectively).

The great structural similarity between the representative conformation of cluster 1 and the crystal structure of aliskiren (starting conformation for the MD run) is denoted by an 1.4 Å RMSD (Figure 3b). Regarding the representative structures, the calculated energies for system appear similar with values being around -1790.7 Hartrees (Table 3).

The NMR studies combined with the computational results showed that: aliskiren as a flexible molecule adopts both "open" and "closed" conformations, however the extended conformation is dominant. Thus, the X-ray crystallographic structure accounts for all measured NOEs and computational observations, and it can be

rationalized to be used as an initial structure for studying the stability and dynamic properties of aliskiren in the renin environment.

3.2.3 Conformational Properties of Aliskiren in the Receptor Site

The MD simulation of aliskiren inside renin was initiated from the configuration obtained from the crystal structure of the complex (2V0Z). The same initial coordinates were used for the MD run of the apo renin. Minor initial conformational changes of the protein were observed during the first half of the simulation, which eventually resulted in a converged trajectory. The high degree of stability for the complex is indicated by the consistency of structural deviations during the simulation (Figure 4, red). A Cα-based RMSD calculation with respect to the crystal structure of the complex yielded an average value of ≈1 Å suggesting that the simulated structure equilibrates towards conformations that resemble the crystal structure. Furthermore, it is shown that the simulation presented moderate fluctuations around a stable average structure. As expected, the unbound renin appears more flexible and with a higher deviation from the crystal structure (RMSD ≈ 1.65 Å, Figure 4, black) than the bound system, yet considerably stable.

Hydrogen bonding analysis on the MD trajectory of the complex attributes the high stability of the system to a strong HB network between aliskiren and active site residues of renin. At least five HB interactions that exist throughout the simulation stabilize aliskiren inside renin in a bound structure. Active site residues Asp32/215 and Gly34 are primarily involved in binding aliskiren inside the cavity, while Tyr14, Arg74 and Ser76 further contribute to the strengthening of the interaction. HB interactions as % occurrence during the simulation are summarized in Table 4 and are represented in Figure 5.

Although aliskiren interacts constantly with the binding-cavity residues, the HB rearrangements shown in Table 4 resulted in a relatively flexible inhibitor as denoted by the RMS deviations (Figure 6). This may have contributed to the minor structural changes induced to the complex. Considering the RMS deviations for active site residues Asp32/215 and Gly34, we observe that the structural changes associated with HB formation resulted in an increased stability of the active site that renders the catalytic system as the favorable candidate for substrate-protein interactions. (Figure 7).

Even though the conformation of aliskiren-renin complex remained relatively stable during the simulation, certain regions of the protein presented differences in flexibility. Cα atomic fluctuation calculations for each amino acid of renin revealed that residues such as Ser159, Glu160, Ser161, Gln162, Leu241 and Phe242 appear increasingly flexible (they belong to water exposed regions of the protein that have no interaction with aliskiren), whereas all active site residues belong to the most stable region of the protein with average fluctuations well below 1 Å (Figure 8 and Table 5). The flexibility of residues 152-155 and 239-246 may have additionally contributed to the aforementioned structural changes observed for renin (Figure 4). As expected, compared to the aliskiren-bound form of renin, the corresponding residues of the apo renin appear significantly more mobile, thus further denoting the role of aliskiren in facilitating a stable structure for the complex. Although the active site in the apo form of the protein also appears highly stable, it is further stabilized by the presence of aliskiren due to the formation of hydrogen bonds (Table 5). Active site residues that do not present HB interactions (eg. Gly217, Thr216) appear as stable as before binding to aliskiren.

An important feature emerges after considering residues in the vicinity of Ser76 (Arg74-Tyr75-Ser76-Thr77-Gly78). This region forms a loop that lies on top of the active site, thus covering aliskiren inside the binding pocket of renin. The loop remains attached to aliskiren via two HB interactions (with Arg74 and Ser76) that stabilize the structure (Figure 5). Interestingly, in the apo form of renin, the loop appears increasingly flexible (Table 5), a feature that implicates this region as a modulating factor for the entrance of substrates. Access to the binding cavity of the protein may depend on the sufficient opening of the aforementioned loop. Upon binding, the flexibility of the loop greatly diminished, keeping aliskiren entrapped inside the cavity. A putative mechanism regarding the role of the loop is offered in Figure 9. The highly flexible Ser-76 loop in the apo form of renin acquires "open" and "closed" conformations in dynamic equilibrium. Upon aliskiren binding however, the closed form is stabilized in a compact structure via a HB network involving binding-cavity residues, Ser-76 loop, and aliskiren.

3.2.4 MMPBSA Analysis

To estimate the energetic contributions of binding in a reliable and detailed fashion, the MM-PBSA method has been employed to the aliskiren-renin complex. The convergence of the procedure has been achieved for the system after approximately 10 ns, as depicted in Figure S7 (ΔH plot vs. time and ΔG_{vdW} plot vs. time). The MM-PBSA results are summarized in Table 6. Our prediction yielded –12.03 kcal mol^{-1} total binding energy for the complex. This value is in fair agreement with the experimental value (–12.64 kcal mol^{-1}).[55]

The electrostatic contribution to solvation is much larger than the corresponding contribution to the MM energy. The total electrostatic contribution ($\Delta G_{ele}+\Delta G_{PB}$) is

20.1 kcal mol^{-1}. Thus, the unfavorable electrostatic contribution related with solvation (ΔG_{PB} = 51.3 kcal mol^{-1}) is not fully compensated by the favorable contribution (ΔG_{ele} = –31.2 kcal mol^{-1}) to the MM energy. A similar observation has been made by Gouda et al. for the system of theophylline-RNA.[56] The formation of the aliskiren-renin complex is mainly driven by the van der Waals (–35.7 kcal mol^{-1}) and the nonpolar contribution to solvation (–28.1 kcal mol^{-1}). This trend has been verified by studies on other protein complexes.[51,57]

4 Conclusions

1D and 2D NMR experiments were performed to structure elucidate aliskiren and to explore its conformational properties in DMSO environment. Details on its conformational properties were achieved by using random sampling and molecular dynamics calculations. The best fit after performing conformational analysis agreed with the extended reported crystallographic structure of aliskiren, docked on the binding site. This allowed MD calculations to use this structure as an initial one to study the flexibility and molecular basis interactions in the active site. The MD analysis revealed the stability of aliskiren into the cavity and an existence of a loop around Ser76 that determines its entrance. To our knowledge, this is the first reported evidence for such a loop playing an active role in the incorporation of aliskiren into the active site. Molecular mechanics Poisson–Boltzmann calculations predicted the total free energy of binding for the complex to be –12.0 kcal mol^{-1}, in agreement with the experimental value (–12.6 kcal mol^{-1}). Additionally, it was revealed that the main favorable contributions towards the complex formation were nonpolar and van der Waals interactions. This information directs us to understand the way renin inhibitors

are acting and the application of rational design of new molecules. This work will be a subject of a following publication. Research work is also in progress, where the conformational analysis of aliskiren is studied in micelle and liposome environment in order to reveal its conformational properties in a more biologically-simulated environment. The dynamic properties of the derived conformations in these environments will be compared with those obtained in DMSO solvent and other solvents with different dielectric constants (i.e. CD_3OD). It will be of paramount importance to establish that loop around Ser76 guides the entrance of aliskiren and its active derivatives independently of the starting conformation, an unknown and important parameter to be considered in the binding process.

Acknowledgements: The NMR studies were supported by EN-FIST Center of Excellence (Dunajska 156, SI-1000 Ljubljana, Slovenia) and Ministry of Higher Education, Science and Technology of Slovenia. T.M. and D.N. are recipients of a grant by East-NMR program. G. L. acknowledges funding provided by the European Commission for the FP7-REGPOT-2009-1 Project 'ARCADE' (Grant Agreement No. 245866). We acknowledge the technical assistance of Dr. E. Zervou in obtaining and processing the NMR data. Finally, the authors acknowledge the pharmaceutical company Novartis for kindly donating us aliskiren.

References

[1] C. M. Tice, *Annu. Rep. Med. Chem*. **2006**, *41*, 155.

[2] M. Paul, A. Poyan Mehr, R. Kreutz, *Physiol Rev*. **2006,** *86*, 747.

[3] J. M. Wood, J. L. Stanton, K. G. J. Hofbauer, *Enzyme Inhib. Med. Chem*. **1987**, *1*,169.

[4] N.A. Powell, F.L. Ciske, C. Cai, D.D. Holsworth, K. Mennen, C.A. Van Huis, M. Jalaie, J. Day, M. Mastronardi, P. McConnell, I. Mochalkin, E. Zhang, M.J. Ryan, J. Bryant, W. Collard, S. Ferreira, C. Gu, R. Collins, J.J. Edmunds, *Bioorg Med Chem* **2007**, *15*, 5912-5949

[5] H. M. Siragy, *Cardiovasc Drugs Ther.* **2011,** *25*, 87.

[6] J. Rahuel, J.P. Priestle, M.G. Grutter, *J. Struct. Biol*. **1991,** *107,* 227.

[7] C. Jensen, P. Herold, H.R. Brunner, *Nat. Rev. Drug Discov*. **2008**, *7*, 399.

[8] J.A. Staessen, Y. Li, T. Richart, *Lancet* **2006**, *368(9545),* 1449.

[9] N.D. Fisher, N.K. Hollenberg, *J Am Soc Nephrol* **2005**, *16*, 592.

[10] M. Azizi, R. Webb, J. Nussberger, N.K. Hollenberg, *J Hypertens* **2006**, *24*, 243.

[11] M.J. Brown, *Circulation* **2008,** *118*, 773.

[12] A. Gradman, R. Schmieder, R. Lins, J. Nussberger, Y. Chiang, M. Bedigian, *Circulation.* **2005,** *111(8)*, 1012.

[13] J.M. Wood , J. Maibaum , J. Rahuel , M.G. Grütter , N.C. Cohen , V. Rasetti , H. Rüger , R. Göschke , S. Stutz , W. Fuhrer , W. Schilling , P. Rigollier , Y. Yamaguchi , F. Cumin , H.P. Baum , C.R. Schnell , P. Herold , R. Mah , C. Jensen, E. O'Brien , A. Stanton , M.P. Bedigian , *Biochem Biophys Res Commun.* **2003,** *308(4)*, 698.

[14] A.P. Politi, S. Durdagi, P.M. Minakakis, T. Mavromoustakos, G. Kokotos, *J. Mol. Gr. Mod*. **2010**, *29*, 425.

[15] A.R. Leach, Molecular Modelling: Principles and Applications. 2nd Edition, **2001**, Pearson Education Ltd

[16] W. Wang , O. Donini , C.M. Reyes , P.A. Kollman , *Annu Rev Biophys Biomol Struct.* **2001**, *30*, 211.

[17] S. Wan, P. V. Coveney, D. R. Flower, *Philosophical Transactions of the Royal Society A: Mathematical, Physical and Engineering Sciences.* **2005**, *363,* 2037.

[18] W. L. Jorgensen, *Science* **2004**, *303*, 1813.

[19] S. A. Adcock, J. A. McCammon, *Chem. Re*v. **2006***, 106*, 1589.

[20] P. A. Bash, U. C. Singh, F. K. Brown, R. Langridge, P.A. Kollman, *Science* **1987**, *235*, 574.

[21] J. Gao, K. Kuczera, B. Tidor, M. Karplus, *Science* **1989**, *244*, 1069.

[22] M. Lawrenz, R. Baron, *J.* A. McCammon, *J. Chem. Theory Comput.* **2009**, *5*, 1106.

[23] W. Wang, P. A. Kollman, , *Proc. Natl. Acad. Sci. U. S. A.* **2001**, *98*, 14937.

[24] Y. Xu, R. Wang, , *Proteins* **2006**, *64*, 1058.

[25] H. Gohlke, C. Kiel, D. A. Case, *J. Mol. Biol.* **2003**, *330*, 891.

[26] Quanta, Molecular Simulations Inc., San Diego, CA, 1997.

[27] B.R. Brooks, R.E. Bruccoleri, B.D. Olafson, D.J. States, S. Swaminathan, M.M. Karplus, , *J Comput Chem.* **1983**, *4*, 187.

[28] M.A.C. Preto, A. Melo, H.L.S. Maia, T. Mavromoustakos, M.J. Ramos, *J. Phys. Chem. B*, **2005**, *109(37),* 17743.

[29] K.P. Soteriadou, A.K. Tzinia, E. Panou-Pamonis, V. Tsikaris, M. Sakarellos-Daitsiotis, C. Sakarellos, Y. Papapoulou, R. Matsas, , *Biochem. J.* **1996**, *313*, 455.

[30] D.A. Case, T.E. Cheatham, T. Darden, H. Gohlke, R. Luo, K.M. Merz, Jr., A. Onufriev, C. Simmerling, B. Wang, R. Woods, *J. Computat. Chem.*, **2005**, *26*, 1668.

[31] D.A. Case, T.A. Darden, T.E. Cheatham III, C.L. Simmerling, J. Wang, R.E. Duke, R. Luo, W. Walker, K.M. Zhang, B. Merz, B. Roberts, S. Wang, A. Hayik, G. Roitberg, I. Seabra, K.F. Kolossváry, F. Wong, J. Paesani, J. Vanicek, X. Liu, S.R. Wu, T. Brozell, H. Steinbrecher, Q. Gohlke, X. Cai, J. Ye, M.-J. Wang, G. Hsieh, D.R. Cui, D.H. Roe, M.G. Mathews, C. Seetin, V. Sagui, T. Babin, S. Luchko, A. Gusarov, Kovalenko, and P.A. Kollman, (2010), AMBER 11, University of California, San Francisco.

[32] J. Rahuel, V. Rasetti, J. Maibaum, H. Rueger, R. Goschke, N.C. Cohen, S. Stutz, F. Cumin, W. Fuhrer, J.M. Wood, M.G. Grutter, *Chem.Biol.*, **2000**, *7*, 493.

[33] J. Wang, R.M. Wolf, J.W. Caldwell, P.A. Kollamn, D.A. Case, *J. Comput. Chem.,* **2004**, *25*, 1157.

[34] A. Jakalian, B.L. Bush, D.B. Jack, C.I. Bayly, *J. Comput. Chem.,* **2000**, *21*, 132.

[35] A. Jakalian, D.B. Jack, C.I. Bayly, *J. Comput. Chem.,* **2002**, *23*, 1623.

[36] T. Fox, P.A. Kollman, *J. Phys. Chem. B*, **1998**, *102*, 8070.

[37] J.A. Izaguirre, D.P. Catarello, J.M. Wozniak, R.D. Skeel, *J. Chem. Phys.*, **2001**, *114*, 2090.

[38] J.P. Ryckaert, G. Ciccotti, H.J.C. Berendsen, *J. Comput. Phys.* **1977**, *23*, 327.

[39] C. Simmerling, R. Elber, and J. Zhang, *Moil-view—A program for visualization of structure and dynamics of biomolecules and STO—A program for computing stochastic paths.* Kluwer, Netherlands, **1995**.

[40] V.A. Rassolov, M.A Ratner, J.A. Pople, P.C. Redfern, L.A. Curtiss, *J. Comp. Chem.*, **2001,** *22*, 976.

[41] M.J. Frisch, H.B. Trucks, G.E. Schlegel, M.A. Scuseria, J.R. Robb, G. Cheeseman, G. Scalmani, V. Barone, B. Mennucci, G.A. Petersson, H. Nakatsuji, M. Caricato, X. Li, H.P. Hratchian, A.F. Izmaylov, J. Bloino, G. Zheng, J.L. Sonnenberg, M. Hada, M. Ehara, K. Toyota, R. Fukuda, J. Hasegawa, M. Ishida, T. Nakajima, Y. Honda, O. Kitao, H. Nakai, T. Vreven, J.A. Montgomery, Jr., J.E. Peralta, F. Ogliaro, M. Bearpark, J.J. Heyd, E. Brothers, K.N. Kudin, V.N. Staroverov, R. Kobayashi, J. Normand, K. Raghavachari, A. Rendell, J.C. Burant, S.S. Iyengar, J. Tomasi, M. Cossi, N. Rega, N.J. Millam, M. Klene, J.E. Knox, J.B. Cross, V. Bakken, C. Adamo, J. Jaramillo, R. Gomperts, R.E. Stratmann, O. Yazyev, A.J. Austin, R. Cammi, C. Pomelli, J.W. Ochterski, R.L. Martin, K. Morokuma, V.G. Zakrzewski, G.A. Voth, P. Salvador, J.J. Dannenberg, S. Dapprich, A.D. Daniels, Ö. Farkas, J.B. Foresman, J.V. Ortiz, J. Cioslowski, D.J. Fox, Gaussian, Inc., Wallingford CT, 2009, Gaussian 09.

[42] ZY. Zhang, I.M. Reardon, J.O. Hui, K.L. O'Connell, R.A. Poorman, A.G. Tomasselli, R.L. Heinrikson, *Biochemistry*, **1991**, *30(36),* 8717.

[43] J.S. Tokarski, and A.J. Hopfinger, *J. Chem. Inf. Comput. Sci*. **1997**, *37*, 779.

[44] V. Hornak, R. Abel, A. Okur, B. Strockbine, A. Roitberg, C. Simmerling, *Proteins*, **2006**, *65*, 712.

[45] J.M. Word, S.C. Lovell, J.S. Richardson, D.C. Richardson, *J. Mol. Biol*. **1999**, *285*, 1735.

[46] R.J. Woods, *J. Comput. Chem.,* **1990**, *11*, 29.

[47] W.L.C Jorgensen, J.D. Madura, R.W. Impey, M.L. Klein, *J Chem Phys.,* **1983**, *79*, 926

[48] P.A. Kollman, I. Massova, C. Reyes, B. Kuhn, S.H. Huo, L. Chong, M. Lee, T. Lee, Y. Duan, W. Wang, o. Domini, P. Cieplak, J. Srinivasan, D.A. Case, T. E. Cheatham, *Acc. Chem. Rev.,* **2000**, *33*, 889.

[49] B. Honig, A. Nichols, *Science*, **1995**, *268*, 1144.

[50] D. Sitkoff, K.A. Sharp, B.J. Honig, *J..Phys. Chem.*, **1998**, *98*, 1978.

[51] I. Stoica, S.K. Sadiq, P.V. Coveney, *J. Am. Chem. Soc.*, **2008**, *130*, 2639.

[52] J. Weiser, P.S. Shenkin, W.C. Still, *J. Computat. Chem.,* **1999**, *20*, 217.

[53] J. Srinivasan, T.E. Cheatham, P. Cieplak, P.A. Kollman, *J. Am. Chem Soc.*, **1998**, *120*, 9401.

[54] W. Wang, O. Donini, C.M. Reyes, P.A. Kollman, *Annu. Rev. Biophys. Biomol. Struct*., **2001**, *30*, 211.

[55] J. Nussberger, G. Wuerzner, C. Jensen, H.R. Brunner, *Hypertension,* **2002**, *39*, e1.

[56] H. Gouda, I.D. Kuntz, D.A. Case, P.A. Kollman, *Biopolymers*, **2003**, *68*, 16.

[57] T. Hou, J. Wang, Y. Li, W. Wang, *J. Chem. Inf. Model.*, **2011**, *51*, 69.

FIGURE LEGENDS

Figure 1: Structure of aliskiren and its critical dihedral angles.

Figure 2: ^{1}H and ^{13}C NMR spectra of aliskiren obtained at 25^{o}C in DMSO-d6 and using 600 MHz Varian NMR spectrometer.

Figure 3: (a) The representative structures of aliskiren produced by the clustering analysis: The dominant, extended form (cluster 1, red) and the closed form (cluster 2, green). (b) Superimposition of the representative structure of cluster 1 (red) with the crystal structure of aliskiren (blue).

Figure 4: RMSD of renin (2V0Z) starting from the crystal structure and overlapped on the same structure. Superpositions of Cα atoms are displayed for: the aliskiren-renin complex (red) and the unbound form of renin (black).

Figure 5: MD results showing hydrogen bonds between aliskiren and renin residues. Eight principal interactions involving active site residues Gly34, Asp32/215 and Tyr14, Arg74, Ser76 stabilize aliskiren inside the protein.

Figure 6: RMSD of aliskiren inside 2V0Z starting from the structure obtained after the equilibration and overlapped on the crystal structure of aliskiren.

Figure 7: RMSD of aliskiren-renin complex starting from the structure obtained from the equilibration and overlapped on the crystal structure. Superpositions of different backbone atoms are displayed: Cα of active site residues (Asp32/215, Thr33/216, Gly34/217) red and Cα of HB-involved residues (Tyr14, Arg74, Ser76) black.

Figure 8: Cα atomic fluctuations of apo renin (black) and aliskiren-renin complex (red).

Figure 9. A putative mechanism involving Ser76 loop (red) as implicated in modulating the entrance of aliskiren inside renin: a) sufficient opening may be required for a substrate in order to access the cavity; b) upon binding, the loop stabilizes the structure by entrapping aliskiren into the binding cavity. Highly mobile solvent-exposed regions of renin (residues 159-162, yellow and 141-144, orange) are also displayed along with the active site (green) and aliskiren in its extended conformation (blue).

Tables

Table 1: 1H NMR assignments of aliskiren obtained in DMSO-d6, using varian 600 MHz at 25 ^{o}C.

Table 2: The most important NOEs observed in aliskiren that determine its conformational properties as quantified.

Table 3: Comparison of experimental (NMR) and theoretical (*ab initio*) distances between protons of aliskiren.

Table 4: Principal HB interactions involving aliskiren and renin.

Table 5. Cα atomic fluctuations (in Å) for the active site residues of the aliskiren-bound and unbound renin.

Table 6. Energy analysis of aliskiren-renin complex (kcal/mol)

SUPPLEMENTARY FIGURE LEGENDS

Figure S1: A representative structure of aliskiren into the binding cavity of renin. Aliskiren in its extended conformation (blue) bound to the active site (Asp32/215, Thr33/216, Gly34/217; green) of renin and covered by the Ser76 loop (red).

Figure S2: 2D COSY of aliskiren obtained in DMSO-d6 at 25 ^{o}C and using 600 MHz varian NMR spectrometer.

Figure S3: 2D NOESY of aliskiren obtained in DMSO-d6 at 25 ^{o}C and using 600 MHz varian NMR spectrometer.

Figure S4: 2D HSQC of aliskiren obtained in DMSO-d6 at 25 ^{o}C and using varian 600 MHz varian NMR spectrometer.

Figure S5: 2D HMBC of aliskiren obtained in DMSO-d6 at 25 ^{o}C and using 600 MHz varian NMR spectrometer.

Figure S6: Six representative, low-energy conformers of aliskiren in DMSO as obtained by random sampling analysis.

Figure S7: MM-PBSA computed results of aliskiren–protease a) binding free energy with respect to the time, and b) van der Waals energy component of binding free energy with respect to the time.

Table S1: Observed HSQC and HMBC correlation in aliskiren.

Table 1

Peaks	*δ(ppm)*	*Number of protons*	*J*
18	0.75	3	6.4
17	0.77	3	6.8
9,10	0.82	6	6.6
3,4	1.00	6	
14	1.20	2	
11β	1.27	1	
16	1.53	1	
11α	1.57	1	
8	1.64	1	
15	1.75	1	
27	1.91	2	
7	2.23	1	
19β	2.32	1	8.5
19α	2.44	1	7.0
13	2.46	1	
12	3.04	1	
5β	3.09	1	5.8
29	3.23	3	
5α	3.28	1	6.7

28	3.45	2	6.3
30	3.70	3	
26	3.95	2	6.7
CH (hemifoumarate)	6.34	1	
21	6.69	1	9.4 (HSQC)
25	6.75	1	
22	6.79	1	9.4 (HSQC)
CONHβ	6.80	1	
CONHα	7.16	1	
NH	7.52	1	6.5

Table 2

Protons		*Distance (Å)*
25	19α/19β	3.04
25	15	3.11
26	25	2.6
12	19α	3.15
12	15	3.0
$CONH_2$	3/4	3.74

Table 3. Comparison of experimental (NMR) and computed (ab initio) distances between protons of aliskiren.

Proton 1	Proton 2	Distance (Å)				Experimental (Å)
		Cluster 1 (implicit DMSO)	Cluster 2 (implicit DMSO)	Cluster 1 (gas)	Cluster 2 (gas)	
25	19a/b	3.18	3.16	3.15	3.20	3.04
25	15	2.58	2.80	2.68	2.68	3.11
25	26	2.90	2.31	2.91	2.90	2.60
12	19a	4.69	5.30	4.68	4.35	3.15
12	15	2.22	4.34	2.19	2.36	3.00
$CONH_2$	3/4	3.63	3.66	3.65	3.60	3.74
MRE		0.18	0.23	0.17	0.16	
Energy (Hartree)		-1790.7324	-1790.7378	-1790.7092	-1790.7121	

Relative Error (RE) = |Calc –Exp|/ Exp.

Mean Relative Error (MRE) = Σ (RE)/ n where n= population size.

Table 4. Principal HB Interactions involving aliskiren and renin.

Interaction	Occurrence	Comment
Amide H' with carbonyl O Gly34	98%	Appears throughout the simulation
Amide H'' with carboxylate OD1 Asp215	97%	Appears throughout the simulation
Etheric O with amide H, Tyr14	91%	Appears throughout the simulation
Hydroxyl O with carboxyl HD2 Asp32	90%	Appears less frequently at the end
Hydroxyl H with carboxylate OD1 Asp215	87%	
Amide H''' with carbonyl O Arg74	68%	Equally distributed
Hydroxyl H with carboxylate OD2 Asp215	57%	Appears mostly during the first ¾ of the simulation
Carbonyl O with amide H Ser76	56%	Appears more frequently at the end

Note: Amide H' refers to the hydrogen atom of the amide group connected to C5 and 6 (Figure 1); amide H'' and amide H''' refer to the groups attached to C13 and C1, respectively; etheric O is located between C29 and C28; hydroxyl O and hydroxyl H are attached to C12; carbonyl O is attached to C6.

Table 5. Cα atomic fluctuations (in Å) for the active site residues of the aliskiren-bound and unbound renin.

	Residue	aliskiren–renin	Apo renin
Active site residues	Asp32	0.39	0.47
	Thr33	0.37	0.47
	Gly34	0.44	0.59
	Asp215	0.48	0.56
	Thr216	0.53	0.59
	Gly217	0.68	0.65
Loop residues	Arg74	0.67	1.11
	Tyr75	0.65	1.18
	Ser76	0.78	1.51
	Thr77	0.94	1.72
	Gly78	0.86	1.32

Table 6. MM-PBSA energies and standard deviations for the aliskiren-renin complex (kcal mol^{-1}).

	Energy	STDV
ΔG_{ele}	-31.24	2.72
ΔG_{vdW}	-35.67	2.88
ΔG_{MM}	-66.91	2.70
ΔG_{NP}	-28.14	2.00
ΔG_{PB}	51.32	2.25
ΔG_{solv}	23.18	2.34
$\Delta G_{ele(TOT)}=\Delta G_{ele}+\Delta G_{PB}$	20.08	3.14
$\boldsymbol{\Delta H}$	-39.23	2.86
$-T\Delta S_{rot}$	8.49	1.67
$-T\Delta S_{trans}$	6.48	1.90
$-T\Delta S_{vib}$	12.23	2.41
$\boldsymbol{-T\Delta S_{TOT}}$	27.20	2.30
$\boldsymbol{\Delta G_{TOT}}$	-12.03	2.22

Figure 1

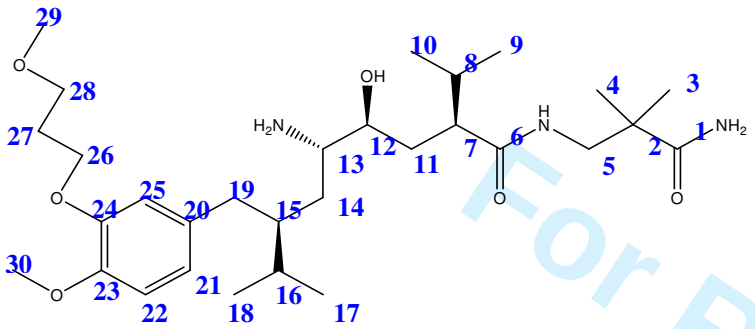

τ_1 : C22 – C23 – O – C30
τ_2 : C21 – C20 – C19 – C15
τ_3 : C23 – C24 – O – C26
τ_4 : C24 – O – C26 – C27
τ_5 : O – C26 – C27 – C28
τ_6 : C26 – C27 – C28 – O
τ_7 : C27 – C28 – O – C29
τ_8 : C28 – O – C29 – H
τ_9 : C27 – O – C30 – H
τ_{10} : C20 – C19 – C15 – C14
τ_{11} : C19 – C15 – C14 – C13
τ_{12} : C19 – C15 – C16 – C18
τ_{13} : C15 – C14 – C13 – C12
τ_{14} : C14 – C13 – C12 – C11
τ_{15} : C14 – C13 – N – H
τ_{16} : C13 – C12 – C11 – C7
τ_{17} : C13 – C12 – O – H
τ_{18} : C12 – C11 – C7 – C6
τ_{19} : C11 – C7 – C6 – N
τ_{20} : C11 – C7 – C8 – C10
τ_{21} : C7 – C6 – N – C5
τ_{22} : C6 – N – C5 – C2
τ_{23} : N – C5 – C2 – C1
τ_{24} : C15 – C16 – C18 – H
τ_{25} : C15 – C16 – C17 – H
τ_{26} : C7 – C8 – C10 – H
τ_{27} : C7 – C8 – C9 – H
τ_{28} : C5 – C2 – C1 – N
τ_{29} : C5 – C2 – C4 – H
τ_{30} : C5 – C2 – C3 – H
τ_{31} : C2 – C1 – N –H

Figure 2

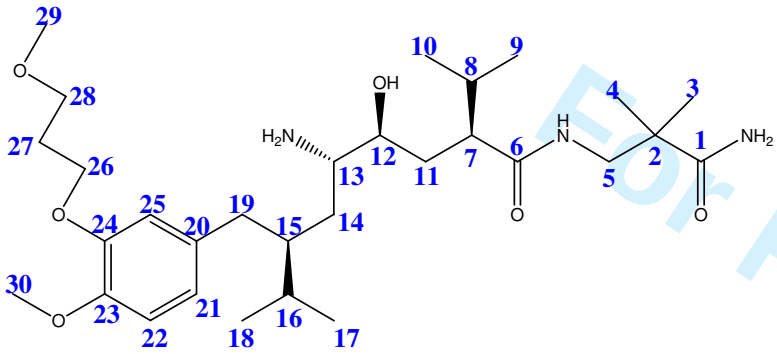

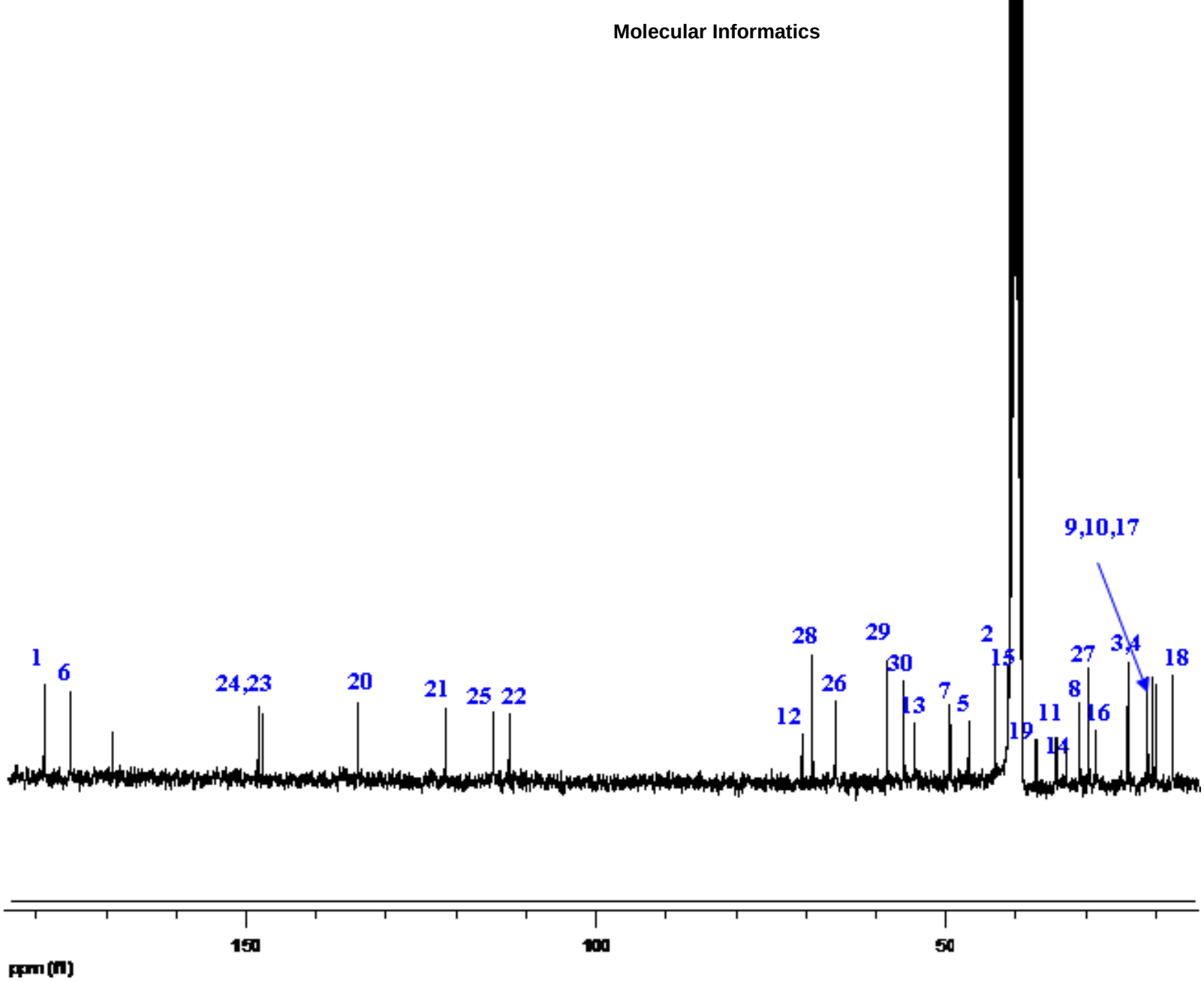
1
6
24,23
20
21
25
22
28
29
30
26
12
13
7
5
2
15
19
11
14
8
16
27
3,4
9,10,17
18
150
100
50
ppm (f1)

Figure 3

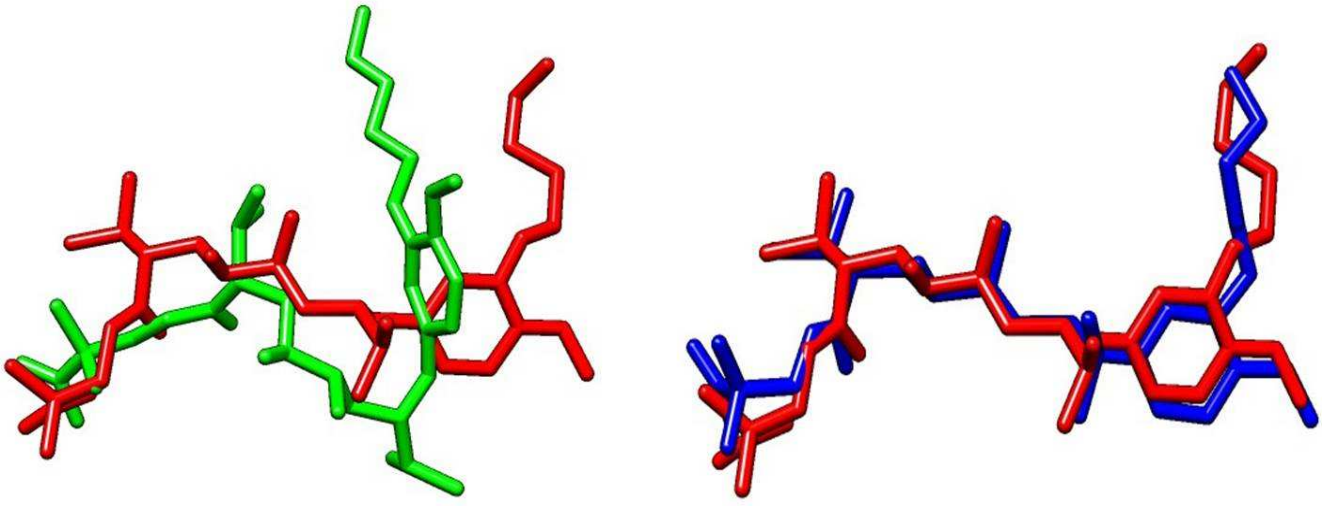

a b

Figure 4

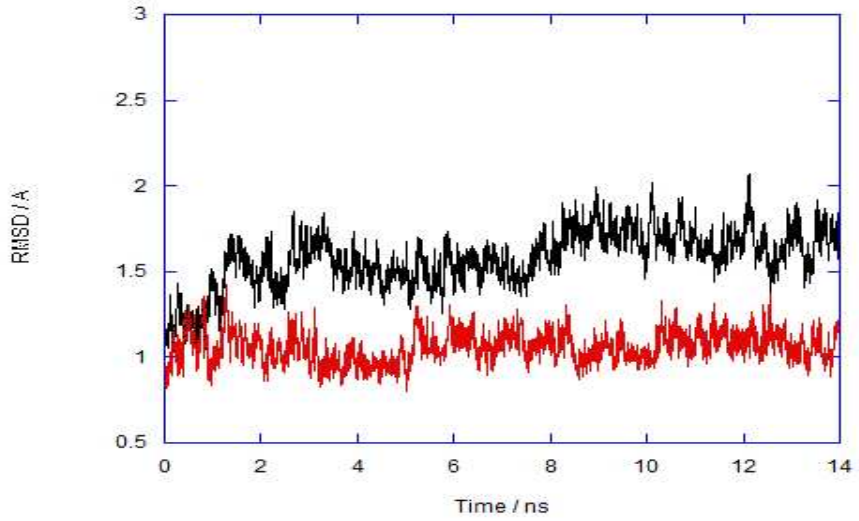

Figure 5

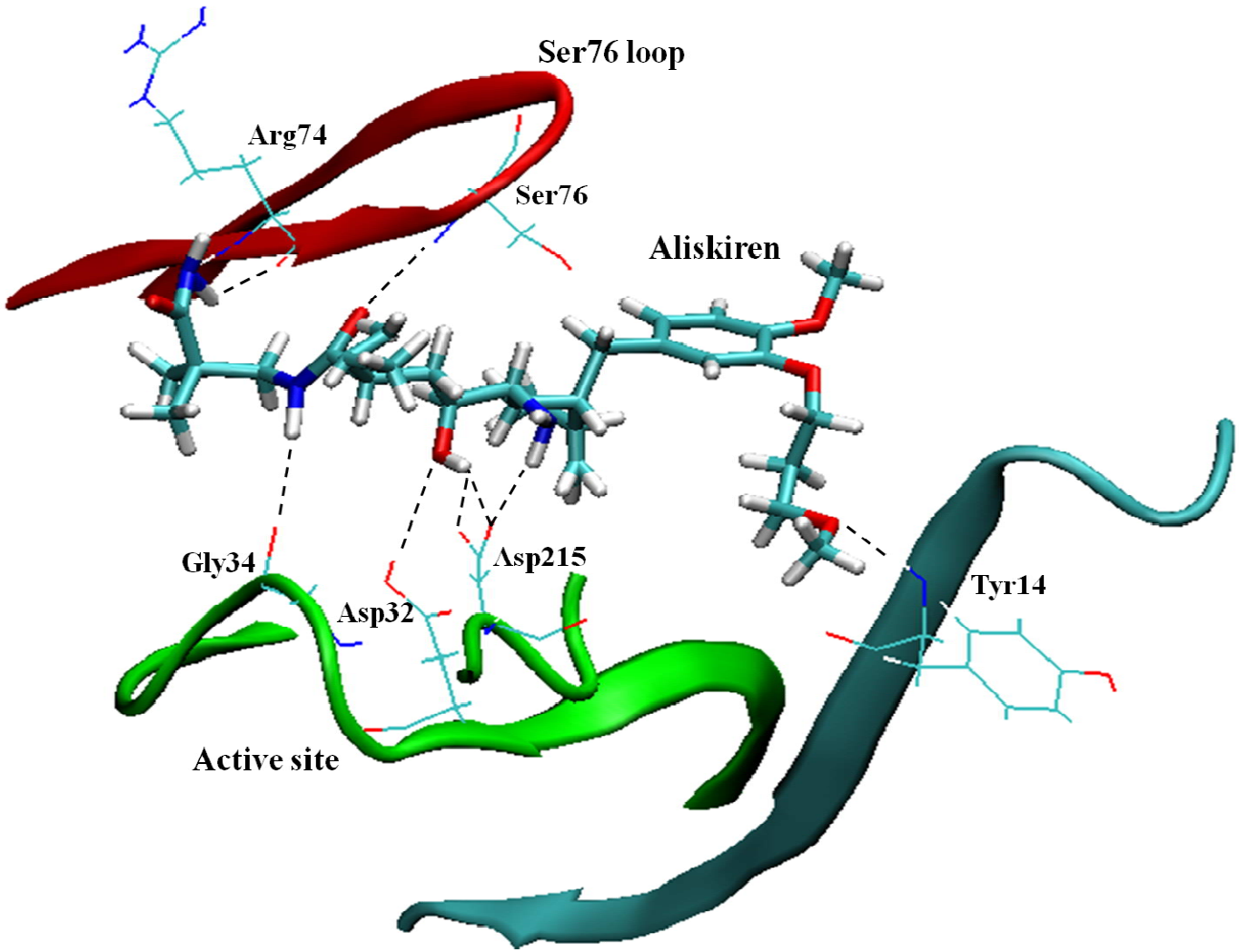
Ser76 loop
Arg74
Ser76
Aliskiren
Gly34
Asp215
Asp32
Tyr14
Active site

Figure 6

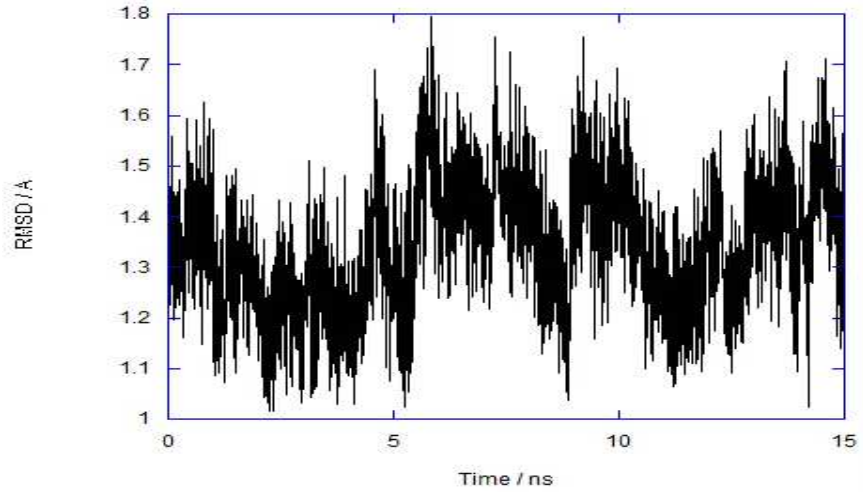

Figure 7

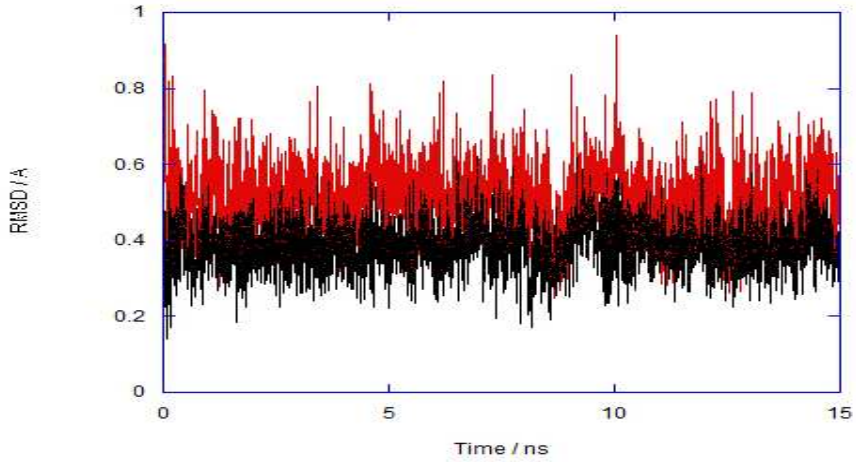

Figure 8

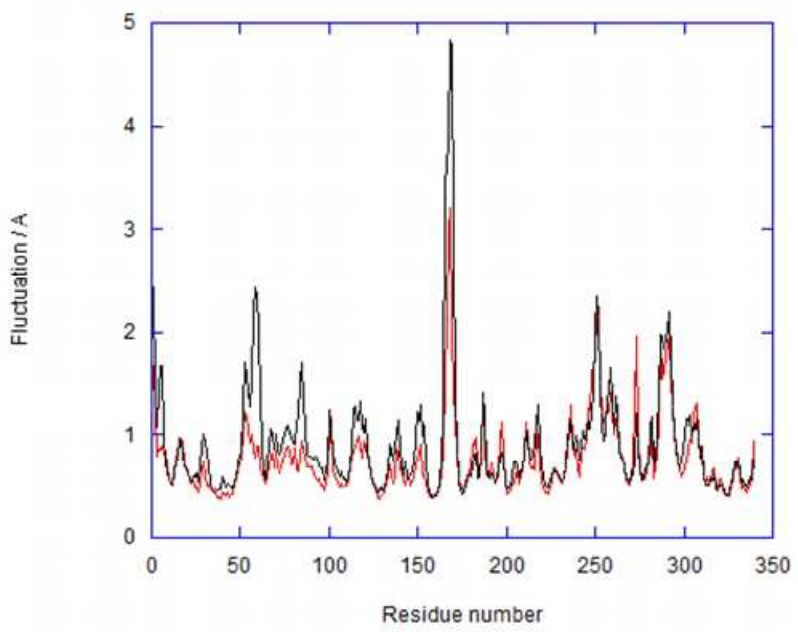

Figure 9